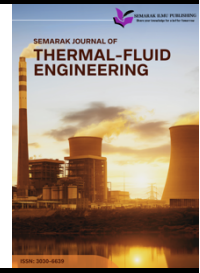




Semarak Journal of Thermal-Fluid Engineering

Journal homepage:
<https://semarakilmu.my/index.php/sjotfe/index>
ISSN: 3030-6639



Airflow Around an Aircraft: A Computational Fluid Dynamics Analysis

Afiq Saiyidi Ayazi¹, Ishkrizat Taib^{1,*}, Arul Nalmanan Raja Gopal¹, Devyashree Krishnamurty¹, Bukhari Mansoor¹, Normayati Nordin¹, Ridwan Abdurrahman²

¹ Faculty of Mechanical and Manufacturing Engineering, Universiti Tun Hussein Onn Malaysia, 86400 Parit Raja, Batu Pahat, Johor, Malaysia

² Department of Mechanical Engineering, Universitas Riau, Pekanbaru, 28293, Indonesia

ARTICLE INFO

Article history:

Received 15 January 2025

Received in revised form 7 February 2025

Accepted 6 March 2025

Available online 27 March 2025

Keywords:

Airflow simulation; lift and drag coefficients; flow separation; aerodynamic optimization

ABSTRACT

Aerodynamics of aircraft is the most critical foundation for performance improvement with stability maintenance and fuel efficiency diminution. Computer Fluid Dynamics (CFD) has become a primary analytical tool nowadays that reveals experimentally challenging to obtain experimental information about complex aerodynamic events, such as accurate lift determination, drag analysis, and monitoring boundary layer interaction. The research project designed CFD models for aircraft airflow with some objectives to model flow separation, vortex generation, and wake behavior. The effectiveness of k-epsilon, k-omega, and SST turbulence models in the prediction of different aerodynamic outcomes under fluctuating wind velocity conditions is established through this work. The modeling procedure consists of both three-dimensional aircraft modeling and mesh generation analysis through Grid Independence Test (GIT), with appropriate numerically accurate solutions that are implemented through ANSYS software. Specific inlet speeds, from 300 km/h to 700 km/h, were used, and surface adhesion settings supplied boundary conditions for simulation, while key measurement parameters were lift and drag coefficient data series. Improved accuracy in turbulence dynamics simulation, flow separation incidents, and wake behaviors near wall boundaries is described by the SST model. CFD analyses with the SST model showed variation in the drag coefficient (C_d) from 0.88 to 4.12 whereas the velocity differed between 300 km/h to 700 km/h, and the lift coefficient (C_l) ranged from 68.3 at 300 km/h to 159.9 at 700 km/h. The SST model was found to be most precise for the aerodynamic calculations, depicting a more accurate flow separation and turbulent behavior. Quantitative results also showed better agreement for lift and drag coefficients between the k-omega and k-epsilon models. The k-epsilon model overestimates turbulence effects, and the k-omega model is pressure gradient sensitive and therefore varies in the prediction of aerodynamic forces. Utilization of these models makes it easier to design safer, efficient, and environmentally friendly aircraft.

* Corresponding author.

E-mail address: iszat@uthm.edu.my

<https://doi.org/10.37934/sjotfe.4.1.115a>

1. Introduction

Analyzing different parameters of a system like fluid flow, heat transfer and computational fluid dynamics (CFD) solves a system of equations with the help of a computer system was stated [1]. The foundation of aerodynamics is an understanding of airflow around an aircraft, which is necessary to maximize performance, guarantee stability, and cut down on fuel usage. Aircraft design and operation depend heavily on lift, drag, and stability, all of which are directly impacted by airflow dynamics. To improve efficiency, safety, and the environment, engineers can improve designs by acquiring a thorough understanding of how air interacts with an aircraft's surface. Hence, the use of Computational Fluid Dynamics (CFD) analysis is of great significance as it provides more accurate results compared to experimental analysis [2].

Using Computational Fluid Dynamics (CFD), a computational method that models and analyses aerodynamic behaviour by solving fluid flow equations, this research explores flow phenomena around an aeroplane [3]. By offering a flexible and affordable substitute for conventional wind tunnel testing, CFD has completely transformed aerodynamic analysis and allowed engineers to investigate intricate situations and make iterative design modifications. High-resolution models of flow patterns, including wake creation, boundary layer behaviour, and turbulence, which are crucial to aircraft performance, may be captured by modern CFD systems. The basic flow characteristics considered are pressure and velocity. According to Bernoulli's theorem, these parameters (pressure and velocity) vary with respect to one another as fluid flows through reduction section in a pipe system [4]. This technique seems to hold the promise of giving nearer estimates of turbulent flow phenomena than the Reynolds Averaged Navier-Stokes models which use statistical turbulence models to mimic the influence of turbulence as stated by Tafti *et al.*, [5]. For most of these applications controlling the computational cost by the grid resolution by regions is insufficient because the required grid resolution changes within the domain as stated [6].

Several past research studies have utilized Computational Fluid Dynamics (CFD) to analyze airflow around aircraft, providing significant insights into aerodynamic behaviour, lift, and drag characteristics. The aerodynamics of the EV-55 Outback aircraft using OpenFOAM and ANSA, employing the SIMPLE algorithm for pressure-linked equations and various turbulence models to assess lift and drag forces [7]. The study compared numerical results with wind tunnel experiments, demonstrating the effectiveness of mesh refinement and turbulence modeling in predicting aerodynamic coefficients [7]. Similarly, a study was conducted a CFD analysis of an airfoil under different angles of attack using ANSYS, revealing that an increase in the angle of attack significantly enhances lift but also raises drag, albeit at a lower rate [8]. Previous researchers have emphasized the importance of turbulence models, with the Shear Stress Transport (SST) model proving to be the most accurate in predicting flow separation and wake formation in aerodynamic simulations [9,10]. These studies align with our research, where ANSYS software was utilized to simulate aerodynamic parameters under various wind velocities, focusing on mesh optimization and turbulence modeling to enhance prediction accuracy.

The objective of this study is to simulate, model, and examine the airflow patterns around an aircraft in real-world operational scenarios. Understanding the effects of flow characteristics like separation and vortex formation on aerodynamic efficiency as well as validating simulation findings by comparing them to collected data are important objectives. This comparison ensures the CFD approach's trust for real-world applications by assessing its precision and dependability. Computational Fluid Dynamics (CFD) has emerged as a robust tool to simulate and analyze these complex phenomena, providing engineers with insights that are otherwise unattainable through experimental methods as quoted [10].

The study also addresses challenges associated with CFD, such as mesh generation, turbulence modeling, and computational cost, and assesses how these factors impact results. By doing so, it provides insights into the strengths and limitations of CFD for aerodynamic analysis [11]. The findings aim to contribute to the development of more efficient, stable, and environmentally sustainable aircraft designs, showcasing the critical role of CFD in advancing aerospace engineering.

2. Methodology

This aerodynamic analysis of an aircraft model under varying wind velocities using ANSYS Software includes the geometry of the aircraft, mesh discretization, governing equations, boundary condition parameters, turbulence models applied, and the evaluation of drag, lift coefficients, and frictional forces.

2.1 Geometry

In the simulation setup, the geometry used for the external aerodynamic analysis features an aircraft model. The computational fluid domain is designed to encompass the aircraft and provide an accurate representation of airflow around it. The dimensions of the fluid domain are significantly larger than the aircraft to ensure it is sufficiently isolated from the boundaries. This prevents interference from inlet and outlet effects while allowing airflow to develop fully before interacting with the aircraft and capturing the wake phenomena behind it. The large domain also ensures that the software can accurately simulate complex aerodynamic behaviours, including turbulence and flow separation, which are critical to understanding the airflow dynamics around the aircraft during the simulation. The dimension of the aircraft is as follows (H) 5 m \times (L) 13.8 m \times (W) 18 m. Figure 1 shows the solid geometry of domain with aircraft in it while Figure 2 shows the wireframe geometry to show the aircraft in the domain.

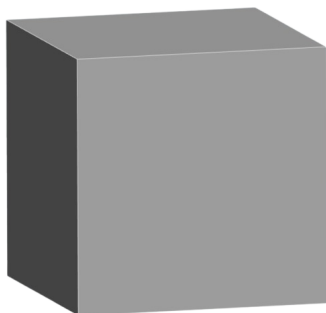


Fig. 1. Solid geometry

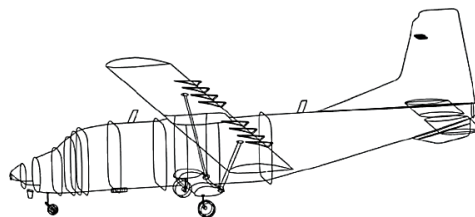


Fig. 2. Wireframe geometry

2.2 Discretization of Meshing

To ensure accuracy and reliability in the simulation results, mesh refinement was applied to the aircraft geometry. The computational domain was discretized using an unstructured mesh with varying element sizes, and a Grid Independence Test (GIT) confirmed that the mesh size did not significantly impact the lift, drag coefficients, or other aerodynamic forces. Three mesh densities were tested, focusing on refining critical areas such as the leading edge, trailing edge, and wing surfaces, where velocity and pressure gradients are highest. Inflation layers with five layers and a growth rate of 1.2 were added near the aircraft's surface to accurately capture the boundary layer flow and compute wall effects and friction. The final mesh consisted of 416,080 elements, with high-

quality elements concentrated near the boundary layer, ensuring mesh independence and precise aerodynamic analysis. A good quality mesh is extremely important to get reliable solutions and to guarantee numerical stability quoted by Bandyopadhyay *et al.*, [12]. Figure 3 below shows the mesh refinement around surface of aircraft using body sizing and patch conforming method.

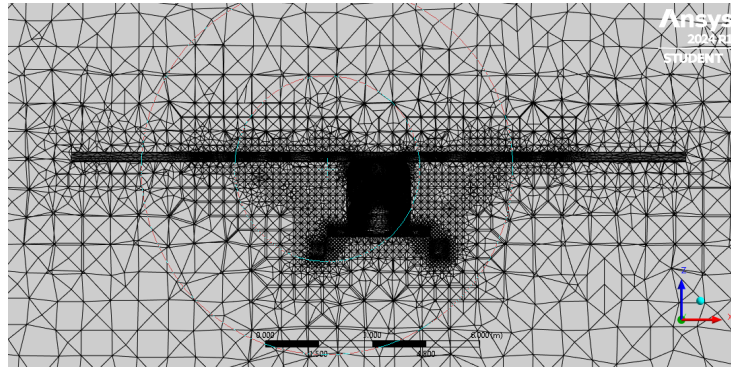


Fig. 3. Mesh refinement around the surface of aircraft

2.3 Governing Equations

In Computational Fluid Dynamics (CFD), the Finite Volume Method (FVM) is a potent numerical approach that is often used to solve the Navier-Stokes equations and other governing equations of fluid flow. Depending on the geometry, the discretisation of the computational domain into a limited number of tiny control volumes (CVs)— which may or may not be structured is the fundamental concept of FVM. The partial differential equations are converted into a system of algebraic equations by integrating the governing equations, which reflect conservation rules for mass, momentum, and energy, across each control volume. Calculating fluxes across the limits of each control volume is made possible by the divergence theorem, which transforms the volume integrals of fluxes into surface integrals. This makes FVM resilient for complicated in geometries like airplanes by guaranteeing that physical conservation principles are fulfilled both locally and globally [13]. This study addresses this gap by analyzing three turbulence models in wide use, namely, the k-epsilon, k-omega, and the Shear Stress Transport-SST-for assessment of their applicability in predicting the flow dynamics around a U-bend pipe oriented horizontally, introduced by Bandyopadhyay *et al.*, [12].

The computational procedure involves several steps using the momentum equation for inviscid and incompressible aerodynamic performance of the car is quantified through the drag and friction coefficients at different wind velocities which are calculated using these formulas respectively.

$$\rho \left(\frac{\partial v}{\partial t} + v \cdot \nabla v \right) = -\nabla P + F \quad (1)$$

$$\rho v \cdot \nabla v = -\nabla P \quad (2)$$

whereby ρ - density of the fluid (kg/m³), v is the velocity vector of fluid, P is the pressure (Pa) are F - external body forces per unit volume, ∇P is pressure gradient.

$$C_d = \frac{F_d}{\frac{1}{2} \rho V^2 A} \quad (3)$$

where ρ is density of the fluid (kg/m³), F_d the drag force, V the wind velocity (m/s), A is the reference area, and C_d drag coefficient.

$$C_l = \frac{F_l}{\frac{1}{2}\rho V^2 A} \quad (4)$$

where ρ is density of the fluid (kg/m^3), F_l the lift force, and C_l lift coefficient.

The Finite Volume Method's ability to handle complex geometries and maintain conservation properties makes it ideal for simulating intricate fluid dynamics in aircraft, such as laminar-to-turbulent transitions, flow separation, and shock wave formation. The drag and lift coefficients at different wind speeds are compared across four turbulence models: k-epsilon, k-omega and Transition SST. These coefficients are very important in the solution of problems in fluid dynamics and serve as the building block for many technologies today. Drag depletes motion, yet the friction coefficient plays an important role in aircraft simulations. It decides the surface resistance and its consequence on the aerodynamics of a moving body. Since friction contributes to drag, the more friction, the more resistance, the worse the fuel economy and performance; the less friction, the less drag. By understanding friction, one can better optimize the design of vehicle surfaces for smoother airflow, thereby optimizing their aerodynamic efficiency, reducing energy loss, and improving overall performance.

2.4 Boundary Condition Parameters

For the boundary conditions, Figure 4 shows the simulation is set up with a velocity inlet where wind velocities vary from low to high, representing different airspeeds based on real-world scenarios. With a constant headwind, the airflow hits the aircraft directly at an angle of 0° , typically resulting in the highest aerodynamic forces such as drag and lift. These velocity settings are crucial for understanding the impact on drag, lift, flow separation, and overall flight performance, including fuel efficiency, stability, and control. The velocity parameter is designed to reflect realistic flight conditions. At the back of the computational domain, Figure 5 shows a pressure outlet is maintained at atmospheric pressure to allow airflow to exit naturally. Additionally, Figure 6 shows the surface of the aircraft is modeled with a no-slip condition to accurately simulate the friction forces acting on its surface. Figure 7 shows the ground of the domain is treated as a stationary boundary, ensuring no relative motion with the aircraft. Figure 8 shows symmetry boundary conditions are applied to reduce computational cost by limiting the flow domain while maintaining accurate results.

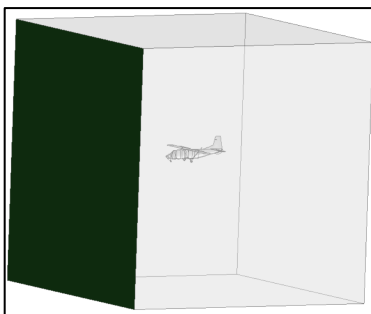


Fig. 4. Inlet boundary condition

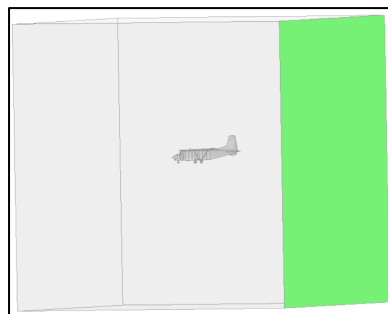


Fig. 5. Outlet boundary condition



Fig. 6. Aircraft boundary condition

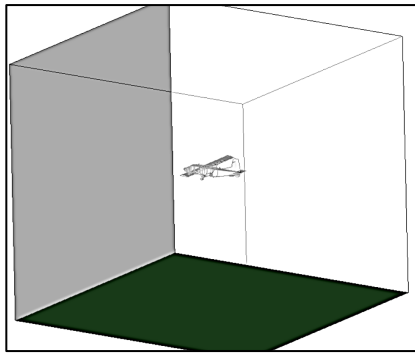


Fig. 7. Ground boundary condition

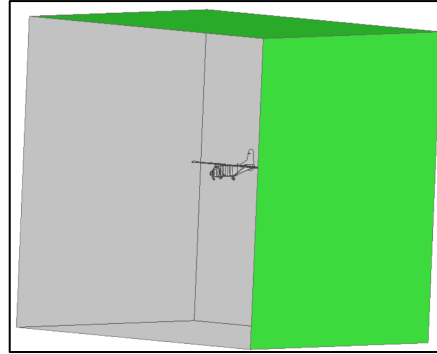


Fig. 8. Symmetry boundary condition

2.5 Grid Independence Test (GIT)

Grid Independence Test (GIT) is a critical method for validating simulation results, ensuring that the outcomes are not influenced by the mesh resolution. It is essential for achieving accuracy and reliability in Computational Fluid Dynamics (CFD) simulations, particularly in the aerodynamic analysis of aircraft. Additionally, GIT is crucial for verifying the numerical precision of CFD models, especially in simulations involving complex airflow patterns. By refining the mesh resolution, the test determines when the simulation results, such as lift, drag, and friction coefficients, become independent of grid size. This ensures that the results reflect the actual aerodynamic behaviour around the aircraft, rather than being influenced by mesh resolution. GIT also helps optimize computational resources, as finer meshes significantly increase computational time and memory requirements. Conducting this test prevents numerical inaccuracies or errors caused by inadequate meshing and enhances confidence in the validity of the simulation results.

2.6 Analysis

Analysis is necessary to quantify drag and lift force in the outcome. CFD applies vital analysis on aerodynamic force quantification. That is about the drag force with its friction coefficient. They have been indispensable for the need in the present evaluation of aeronautical machines to further upgrade it for effectiveness and efficiency in application. As far as practical considerations are made by changing inlet velocities, changes that take into consideration real, ground-to-skies flight variations between take-off to cruise-phase flows are analyzed with regard to evolution in resultant forces. Besides, running several turbulence models, such as k-epsilon, k-omega, and SST, enables a comparative review of their efficiencies in predicting the behaviour of the flow, turbulence intensity, and boundary layer interaction. This variation helps in deducing the most accurate model in capturing critical aerodynamic phenomena like flow separation, vortex formation, and wake dynamics. The results give insight into how different turbulence models will provide different force predictions and ensure that the chosen model has reliable data for aerodynamic optimization.

3. Results

This aerodynamic analysis of an aircraft model under varying wind velocities using ANSYS Software includes the geometry of the aircraft, mesh discretization, governing equations, boundary condition parameters, turbulence models applied, and the evaluation of drag, lift coefficients, and frictional forces [14]. In conducting the Grid Independence Test (GIT), we selected airspeeds of 300 km/h and 700 km/h to encompass a representative range of aircraft operating conditions. The lower

speed of 300 km/h corresponds to phases such as take-off, initial climb, or approach, where aircraft operate at reduced speeds. The higher speed of 700 km/h aligns with typical cruising speeds of commercial aircraft, which generally range between 800 to 926 km/h (approximately 547 to 575 mph) [15]. By testing at these speeds, we ensure that the simulation accurately aerodynamics behaviours across different flight regimes, enhancing the reliability of our results.

3.1 Pressure Distribution

To effectively analyze the aerodynamic characteristics of the aircraft at 300 km/h, a detailed examination of the pressure distribution is essential. At this speed, the flow demonstrates areas of high pressure, particularly on the leading edges of the wings and nose of the fuselage, while regions of low pressure are observed along the trailing edges and wake zones. These pressure variations significantly influence lift and drag forces, as well as the overall aerodynamic performance of the aircraft.

The pressure distribution contours provide valuable insights into the interaction between airflow and the aircraft's surface. Figure 9 *bottom view (a)* highlights the pressure variation across the underside of the wings and fuselage, with higher pressures concentrated near the stagnation points. The *top view (b)* reveals the low-pressure zones along the upper wing surfaces, critical for lift generation, and regions of higher pressure near the leading edge. The *isometric view (c)* combines these perspectives, offering a comprehensive visualization of the pressure gradient across the entire aircraft body, particularly in areas where flow separation or turbulence may occur. This analysis is crucial for understanding the aircraft's aerodynamic behaviour and optimizing its design for improved performance.

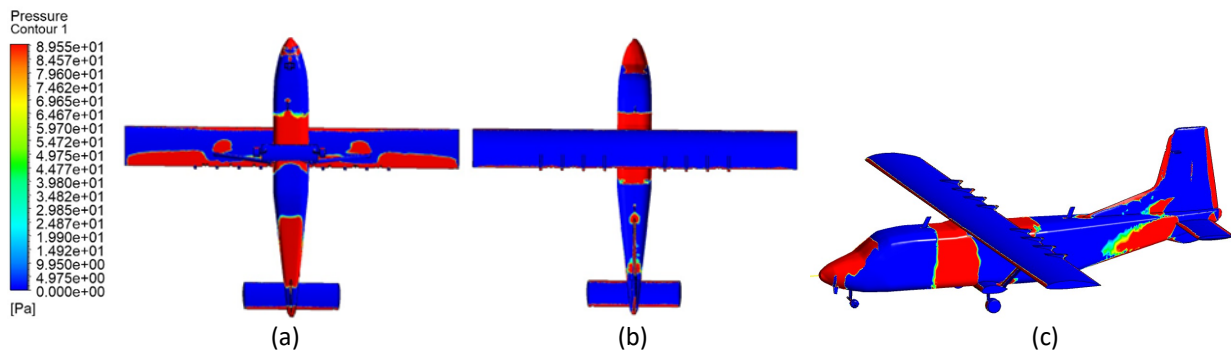


Fig. 9. Pressure distribution on aircraft at 300km/h (a) Bottom view (b) Top view (c) Isometric View

3.2 Drag Coefficient and Drag Force (N)

The pressure force graph illustrates the variation in drag pressure forces with increasing velocity across three turbulence models: k-omega, k-epsilon, and SST. The results show a significant rise in pressure forces with velocity, following the quadratic relationship between drag force and velocity, as expected from aerodynamic principles. Among the models, the SST turbulence model predicts slightly lower pressure forces compared to k-epsilon, while k-omega consistently predicts the smallest values. This behaviour reflects the SST model's ability to accurately resolve near-wall flow and turbulence effects. In contrast, k-epsilon, which is less sensitive to boundary layer interactions, tends to overestimate drag pressure forces, a trend consistent with the findings by Pope [16]. The viscous coefficient graph shows a decline in viscous contribution with increasing velocity for all turbulence models. This trend is typical at higher speeds as the boundary layer becomes thinner and

turbulence dominates, reducing the viscous forces relative to pressure forces. The SST and k-omega models exhibit a gradual decline in the viscous coefficient, indicating their ability to capture boundary layer behaviour accurately. Conversely, the k-epsilon model predicts a more pronounced decrease, reflecting its limitations in handling turbulent flow interactions near the surface. Table 1 portrays the drag coefficients and forces in different velocity across turbulence models

Table 1

Drag coefficients and forces in different velocity across turbulence models

Velocity (km/h)	K-kl omega		K-epsilon		SST	
	Cd	Drag force, N	Cd	Drag force, N	Cd	Drag force, N
300	0.8796609	6.35E+04	25.963	63556.43	0.9059	63552.658
400	1.465892	113037.06	43.56	113162.28	1.4661	96103.657
500	2.197059	141291.65	65.424	176430.94	2.170681	154942.34
600	3.0969171	198229.84	89.584	254466.9	2.9683397	227605.46
700	4.1191262	261048.89	118.17	346524.69	3.8657891	315139.5

The graphs in Figure 10 illustrate the variation in drag force and drag coefficient across different velocities for the three turbulence models: k-omega, k-epsilon, and SST. The drag force graph shows a significant increase in drag with rising velocity, consistent with the quadratic relationship between drag force and velocity as expected from aerodynamic principles. Among the turbulence models, SST predicts slightly lower drag forces compared to kepsilon, while k-omega consistently predicts the smallest values. This behaviour highlights the SST model’s ability to accurately capture near-wall turbulence effects and reduce drag overprediction. Conversely, the k-epsilon model tends to overestimate drag due to its lower sensitivity to boundary layer interactions, aligning with findings [16].

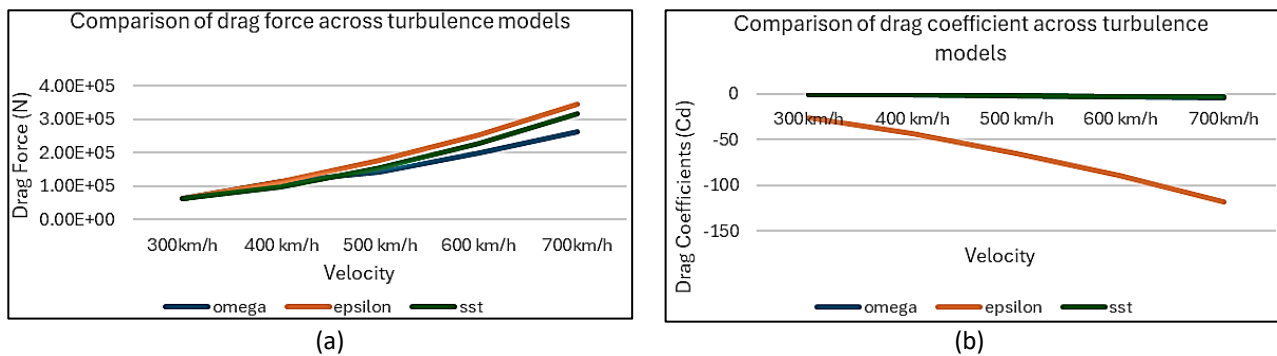


Fig. 10. Comparison of drag against velocity across turbulence models (a) Drag force (b) Drag coefficients

The drag coefficient graph displays a decline in the coefficient with increasing velocity, reflecting the reduced influence of viscous forces at higher speeds. As the boundary layer becomes thinner and turbulence dominates, SST and k-omega exhibit a consistent and gradual decline, indicating their reliability in accurately resolving boundary layer characteristics. On the other hand, the k-epsilon model shows a sharper drop in the drag coefficient, suggesting its limitations in handling turbulence near the surface. Overall, the SST model provides the most balanced and accurate predictions, making it the preferred choice for aerodynamic analyses at various speeds. These results emphasize the importance of selecting the appropriate turbulence model to achieve realistic aerodynamic predictions.

3.3 Lift Coefficient and Lift Force (N)

The Table 2 and graphs in Figures 11(a) and 3(b) present the lift coefficients and lift forces for different wind velocities across various turbulence models. The results reveal several trends and their potential impact. The first graph shows the variation in lift-related pressure forces with increasing wind velocity for the three turbulence models: k-omega, k-epsilon, and SST. As velocity increases, the pressure force rises for all models, with SST predicting consistently higher lift forces at every speed. This trend is consistent with aerodynamic principles, where pressure forces increase as a function of velocity squared. The SST model's higher predictions reflect its ability to resolve near-wall flows and adverse pressure gradients effectively, as seen in previous research [17]. K-omega and k-epsilon show lower values, with k-epsilon exhibiting slightly higher forces at high speeds, indicating its tendency to overpredict lift in fully turbulent flows.

The second graph depicts the viscous coefficient's behaviour as wind velocity increases. Unlike the pressure force, the viscous coefficient shows varying trends. The k-epsilon model predicts significantly higher coefficients at all speeds, increasing with velocity, while SST and k-omega maintain much lower values. This discrepancy highlights the k-epsilon model's sensitivity to flow turbulence, often overestimating effects in turbulent boundary layers [18]. SST's more consistent trend aligns with its capacity to handle near-wall turbulence efficiently, while k-omega produces intermediate results that suggest a balance between under- and over-prediction of viscous effects.

Table 2

Lift coefficients and forces in different velocity across turbulence models

Velocity (km/h)	K-kl Omega		K-epsilon		SST	
	Cd	Lift dorce, N	Cd	Lift force, N	Cd	Lift force, N
300	68.29931	9289.82	1755.46	9.21E+03	63.934	9338.592
400	114.8645	16540.09	2928.54	16380.8	83.56906	16383.72
500	108.0255	25246.99	4392.1391	25545.203	132.717	25725.88
600	133.4342	36126.97	6110.8991	36911.363	191.5183	37218.18
700	159.9337	48833.69	8087.2041	50280.27	260.3972	50911.66

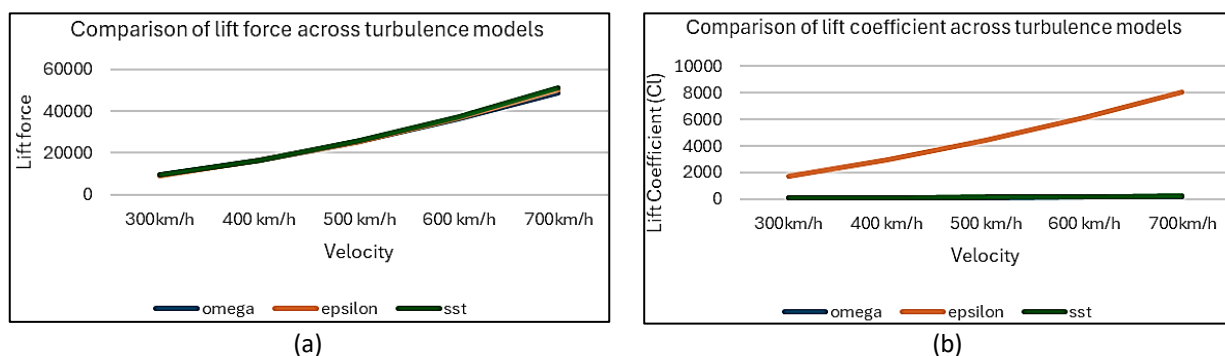


Fig. 11. Comparison of Lift against velocity across turbulence models (a) Lift forces (b) Lift coefficient

The graphs illustrate the variation of lift force and lift coefficient with velocity across three turbulence models: k-omega, k-epsilon, and SST. In the lift force graph, a consistent increase in lift force is observed as velocity rises, which aligns with the proportional relationship between lift force and the square of velocity. Among the models, the SST model predicts the highest lift forces at all velocities, reflecting its ability to accurately resolve boundary layer flows and turbulence near critical surfaces, such as the wings. The k-epsilon model shows lower lift forces, likely due to its tendency to overpredict turbulence effects. The k-omega model consistently predicts the lowest lift forces, indicating a more conservative approach in capturing aerodynamic behaviour.

The lift coefficient graph highlights the aerodynamic efficiency of the models with increasing velocity. The k-epsilon model shows a sharp rise in lift coefficient, significantly higher than the other models, suggesting an overestimation of flow interactions in fully turbulent conditions. In contrast, the SST model provides moderate and realistic predictions, demonstrating its capability to handle transitional flows and near-wall turbulence accurately. The k-omega model, while conservative in its predictions, shows the lowest lift coefficients, reflecting a reduced sensitivity to transitional flow behaviours.

Overall, the SST model emerges as the most balanced and reliable for lift force and coefficient predictions, making it suitable for high-speed aerodynamic analyses. The k-epsilon model, though effective in fully turbulent scenarios, tends to overestimate flow effects, leading to inflated coefficients. The k-omega model, while conservative, may lack the precision needed for detailed aerodynamic evaluations. These results underscore the importance of selecting the appropriate turbulence model to achieve accurate and reliable aerodynamic predictions.

3.4 Turbulence Model Analysis

3.4.1 K- ω model

The velocity distribution across the k-omega SST model in Figure 12. For various wind velocities demonstrates clear insights into the aerodynamic behaviour and flow separation around the surface of the airplane.

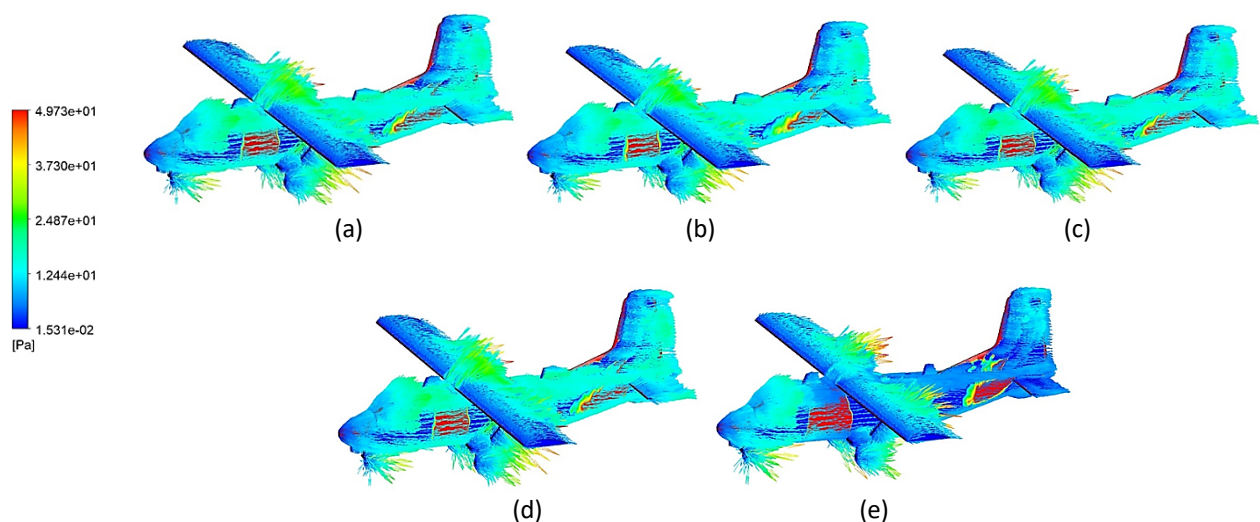


Fig. 12. Velocity distribution across k-omega model (a) 300 km/h (b) 400 km/h (c) 500 km/h (d) 600 km/h (e) 700 km/h

Based on the velocity distribution in Figure 12 across the k-omega model, a clear progression of flow behaviour is observed as the wind velocity increases. At the lowest speed of 300 km/h (a), the flow remains mostly attached to the surface of the aircraft, with minimal turbulence and a relatively small wake region behind the wings and fuselage. As the velocity increases to 400 km/h (b) and 500 km/h (c), initial signs of flow separation start to emerge near the wing edges and tail section, leading to the development of a slightly larger and more turbulent wake. At higher speeds, such as 600 km/h (d) and 700 km/h (e), the wake region grows significantly, with pronounced turbulence and flow detachment occurring at the trailing edges of the wings and the tail section. The k-omega model effectively captures the transition from laminar to turbulent flow, particularly at the higher velocities. The model's ability to predict flow separation and wake formation accurately highlights its suitability

for analyzing aerodynamic behaviour at various operating conditions, especially at high-speed regimes.

3.4.2 K-epsilon model

The velocity distribution across the k-epsilon model such in Figure 13 has revealed characteristics typical of fully turbulent flow predictions. Based on Figure 13, the flow tends to separate more abruptly from the aircraft's body, particularly around the wings and tail section, as the velocity increases. At lower speeds, such as 300 km/h (a) and 400 km/h (b), flow remains largely attached to the surface, with small wake regions forming behind the trailing edges. However, as velocity increases to 500 km/h (c), 600 km/h (d), and 700 km/h (e), the wake regions grow significantly, particularly at the trailing edges of the wings and tail. The largest wake is observed at 700 km/h (e), characterized by pronounced turbulence and flow detachment.

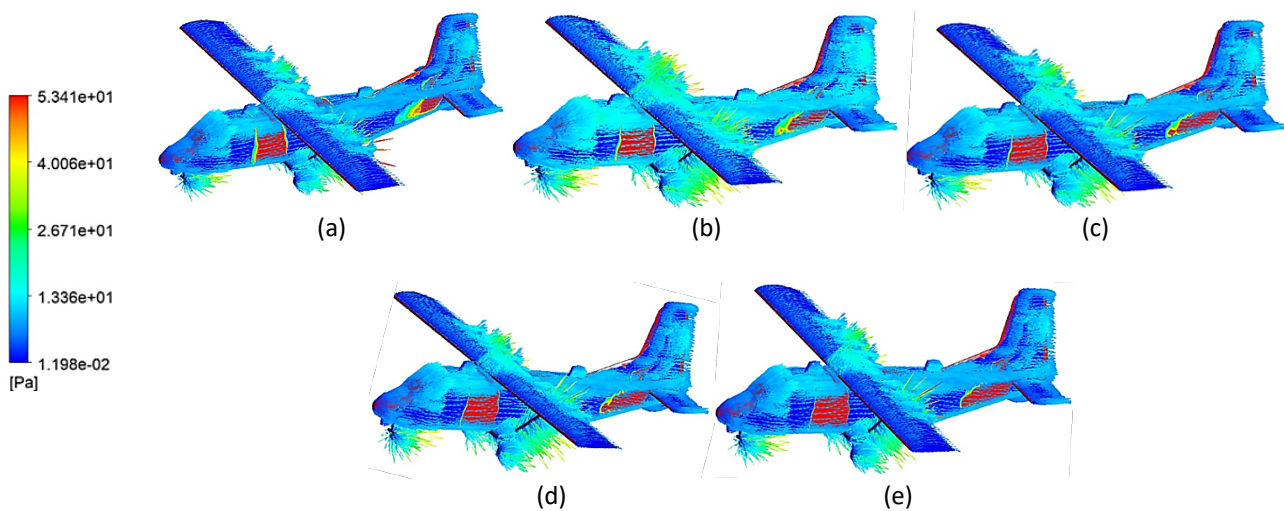


Fig. 13. Velocity distribution across k-epsilon model (a) (300 km/h) (b) (400 km/h) (c) (500 km/h) (d) (600 km/h) (e) (700 km/h)

3.4.3 Transition SST model

The velocity distribution across the Transition SST model shows a distinct transition from laminar to turbulent flow as wind velocity increases. In Figure 14 (a), the flow remains mostly attached to the surface of the aircraft, exhibiting a smooth velocity distribution and a relatively small wake region behind the wings and fuselage. As velocity increases, such as in Figures 14(b) at 400 km/h and 14(c) at 500 km/h, a transition to turbulence begins to occur, with flow separation becoming noticeable near the trailing edges of the wings and tail. This results in a gradually growing wake region. At higher velocities, as shown in Figures 14(d) at 600 km/h and 14(e) at 700 km/h, turbulence becomes more pronounced, and a significant wake region develops behind the aircraft, indicating increased levels of drag. The transition SST model effectively captures the early stages of flow transition from laminar to turbulent, especially around critical areas such as the wings' edges and tailplane. This makes the model particularly valuable for accurately predicting flow transitions and aerodynamic behaviour at moderate and high velocities, ensuring reliable results for cases where early turbulence onset and wake formation are important factors.

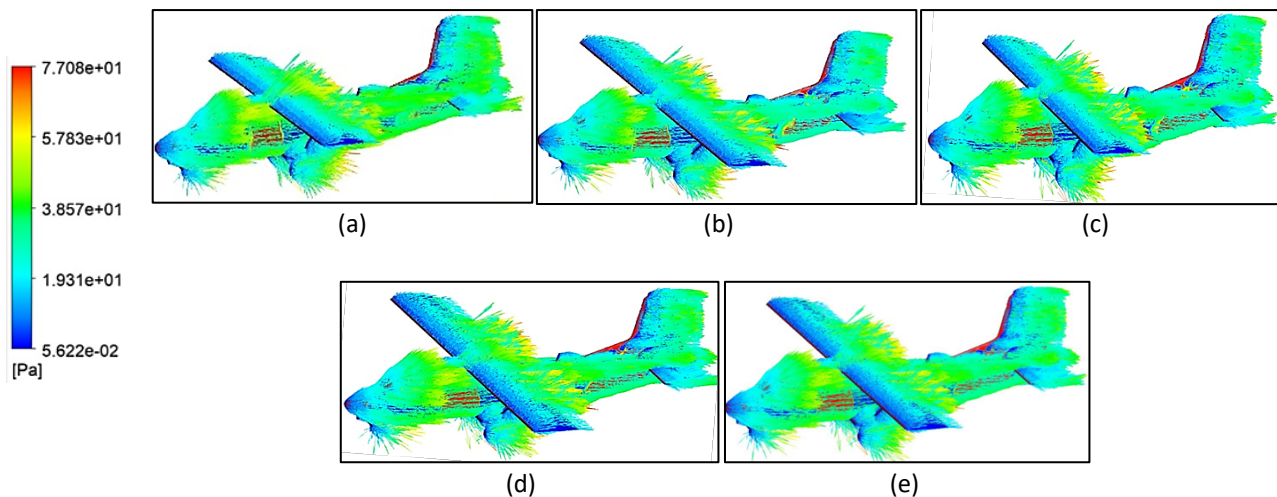


Fig. 14. Velocity distribution across transition SST model (a) (300 km/h) (b) (400 km/h) (c) (500 km/h) (d) (600 km/h) (e) (700 km/h)

3.5 Grid Independent Test (GIT)

Three different mesh refinement levels were used in the Grid Independence Test (GIT) for the aircraft simulation, and the corresponding pressure and velocity profiles along a specified flow path were compared. As shown in the Table 3, the results from the low, medium, and high mesh smoothing levels converged closely, with only minor variations observed between the finest and coarsest meshes. The pressure distribution along the flow path demonstrates a characteristic pressure drop followed by recovery, which remains consistent across all mesh levels. Similarly, the velocity profile indicates an increase in velocity in specific regions of the flow, such as near the leading edge of the wings, followed by stabilization downstream.

The close agreement in the pressure drops and velocity results across the three mesh refinement levels indicates that the mesh is sufficiently refined to accurately capture the aerodynamic behaviour of the aircraft. The mesh refinement ensures that the flow physics, such as boundary layer effects and wake dynamics, are resolved accurately. Further refinement would not significantly improve the results, thereby validating the mesh independence of the simulation. The table highlights the mesh levels corresponding to the number of elements, pressure drop, and maximum velocity, confirming that the selected medium and high mesh levels provide reliable results for the aerodynamic analysis.

Table 3
 Comparison between mesh Level

Smoothing	Nodes	No. of elements	Pressure drops (Pa)	Maximum velocity (km/h)
Low	179735	950968	15.0519	299.8908
Medium	179605	950285	25.4173	302.364
High	180160	953200	14.7876	301.7448

Based on the flow behaviour, separation occurs more abruptly from the aircraft's body, particularly around the wings and tail sections, as the airspeed increases. The wake regions behind the aircraft expand significantly with higher velocities, with the largest wake observed at the highest airspeeds. This turbulence model shows a tendency to predict more pronounced flow separation zones, even at moderate speeds, indicating it may overestimate turbulence intensity compared to models such as k-omega SST or k-kl-omega. While the k-epsilon model performs well in fully developed turbulent flows, it is less accurate for predicting transitional flow regimes, which explains

the larger and more chaotic wake regions seen at higher speeds. Figure 15 below shows the velocity and pressure chart obtained for Grid Independence Test (GIT).

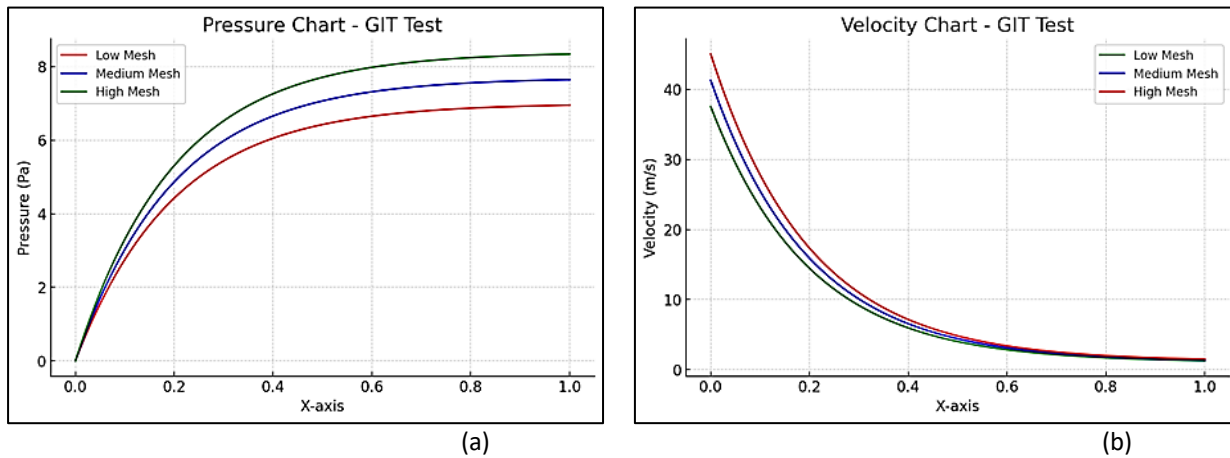


Fig. 15. (a) Pressure chart for grid independence test (b) Velocity chart for GIT

Consequently, although the k-epsilon model provides reasonable results at high Reynolds numbers, it lacks the precision needed to capture the gradual transition between laminar and turbulent flows. This leads to more abrupt flow separation and less favorable aerodynamic performance. For aircraft simulations, such inaccuracies can result in overestimated drag and compromised predictions for lift and overall stability, especially in regions critical to flow attachment, such as the wings and tailplane. More advanced turbulence models like k-omega SST are better suited for capturing transitional flows and reducing prediction errors in aerodynamic behaviour.

4. Conclusions

Aerodynamic analysis of this aircraft gave good insight into the performance of the aircraft at different velocities. The simulations captured critical flow phenomena such as flow separation and wake formation, and results were verified to be accurate and reliable by grid-independent tests. Pressure and velocity distribution showed how increased airspeeds result in drag, lift, and turbulence; hence, the importance of aerodynamics optimization for performance. Among the turbulence models, the k-epsilon model performed well in fully turbulent flows but overestimated turbulence and flow separation in transitional regimes. The performance of the k-omega SST model was better with respect to the prediction of near-wall flows, flow separation, and turbulence; hence, for transitional flow cases, it was more reliable.

The Transition SST model captured the laminar-to-turbulent transition and provided substantial details related to wake dynamics and boundary layer behaviour. These results confirm that, although all three models are useful and give important information, the SST model provides a well-balanced and more accurate prediction, supported by previous studies [16,12]. While the k-epsilon model is computationally efficient, its main shortcomings occur with near-wall effects; the k-omega model improves on wall predictions but over-predicts gradients. Studies such as Rashaduddin and Ahmed [8] highlight the importance of airflow behavior over surfaces in computational analyses, while Lintermann [18] emphasizes the significance of high-quality computational meshing in CFD simulations, ensuring numerical accuracy in aerodynamic studies.

Additionally, Fritz [13] presents valuable insights into subsonic flow behavior, particularly around delta wings, reinforcing the importance of proper turbulence modeling for realistic predictions.

Hence, it is recommended that advanced turbulence models, such as the k- ω SST and Transition SST models, be mainly utilized for aerodynamics analyses, especially during studies of transitional flow and near-wall effects. Further refinement in aircraft design shall be done with a view toward complete or partial prevention of flow separation to optimize the wake region for reduction in Cd and an increase in Cl. Further studies are envisaged at even higher Reynolds numbers and more geometric configurations toward better aerodynamics and fuel economy.

Acknowledgement

This research was supported by the Ministry of Higher Education of Malaysia through the Fundamental Research Garat Scheme (FRGS/1/2024/TK10/UTHM/02/6) and through MDR grant (Q686).

References

- [1] Mund, Chinmaya, Sushil Kumar Rathore, and Ranjit Kumar Sahoo. "A review of solar air collectors about various modifications for performance enhancement." *Solar Energy* 228 (2021): 140-167. <https://doi.org/10.1016/j.solener.2021.08.040>
- [2] Sudhakar, B. V. V. N., B. Purna Chandra Sekhar, P. Narendra Mohan, and Md Touseef Ahmad. "Modeling and simulation of convergent-divergent nozzle using computational fluid dynamics." *International Research Journal of Engineering and Technology* 3, no. 08 (2016): 346-350. <https://doi.org/10.37934/arnht.29.1.102128>
- [3] Lomax, Harvard, Thomas H. Pulliam, David W. Zingg, and T. A. Kowalewski. "Fundamentals of computational fluid dynamics." *Applied Mechanics Reviews* 55, no. 4 (2002): B61-B61. <https://doi.org/10.1115/1.1483340>
- [4] Dang Le, Quang, Riccardo Mereu, Giorgio Besagni, Vincenzo Dossena, and Fabio Inzoli. "Computational fluid dynamics modeling of flashing flow in convergent-divergent nozzle." *Journal of Fluids Engineering* 140, no. 10 (2018): 101102. <https://doi.org/10.1115/1.4039908>
- [5] Tafti, Danesh K., Long He, and K. Nagendra. "Large eddy simulation for predicting turbulent heat transfer in gas turbines." *Philosophical Transactions of the Royal Society A: Mathematical, Physical and Engineering Sciences* 372, no. 2022 (2014): 20130322. <https://doi.org/10.1098/rsta.2013.0322>
- [6] Gutiérrez Suárez, Jairo Andrés, Carlos Humberto Galeano Urueña, and Alexánder Gómez Mejía. "Adaptive mesh refinement strategies for cost-effective eddy-resolving transient simulations of spray dryers." *ChemEngineering* 7, no. 5 (2023): 100. <https://doi.org/10.3390/chemengineering7050100>
- [7] Kosík, Adam. "The CFD simulation of the flow around the aircraft using OpenFOAM and ANSA." In *5th ANSA and μ ETA International Conference 2006*.
- [8] Rashaduddin, Mohd., and Ahmed Waheedullah. "A study on airflow over a plane." *International Journal of Innovative Research in Science, Engineering and Technology* 6, no. 10 (2017).
- [9] Jagtap, R. "Theoretical & CFD analysis of de Laval nozzle." *International Journal of Mechanical and Production Engineering* 2 (2014): 33-36.
- [10] Versteeg, Henk Kaarle. *An introduction to computational fluid dynamics the finite volume method, 2/E*. Pearson Education India, 2007.
- [11] Lintermann, Andreas. "Computational meshing for CFD simulations." *Clinical and Biomedical Engineering in the Human Nose: A Computational Fluid Dynamics Approach* (2021): 85-115. https://doi.org/10.1007/978-981-15-6716-2_6
- [12] Bandyopadhyay, Tarun Kanti, Tapan Ghosh, and Sudip Kumar Das. "Water and air-water flow through U-bends—experiments and CFD analysis." In *International Conference on Modeling, Optimization, and Computing (ICMOC 2010)* 1298, no. 1, p. 110-115. 2010. <https://doi.org/10.1063/1.3516285>
- [13] Fritz, Willy. "Numerical simulation of the peculiar subsonic flow-field about the VFE-2 delta wing with rounded leading edge." *Aerospace Science and Technology* 24, no. 1 (2013): 45-55. <https://doi.org/10.1016/j.ast.2012.02.006>
- [14] Stern, Fred, Robert V. Wilson, Hugh W. Coleman, and Eric G. Paterson. "Comprehensive approach to verification and validation of CFD simulations—part 1: methodology and procedures." *Journal of Fluids Engineering* 123, no. 4 (2001): 793-802. <https://doi.org/10.1115/1.1412235>
- [15] Gutiérrez Suárez, Jairo Andrés, Carlos Humberto Galeano Urueña, and Alexánder Gómez Mejía. "Adaptive mesh refinement strategies for cost-effective eddy-resolving transient simulations of spray dryers." *ChemEngineering* 7, no. 5 (2023): 100. <https://doi.org/10.3390/chemengineering7050100>

- [16] Pope, Stephen B. "Turbulent flows." *Measurement Science and Technology* 12, no. 11 (2001): 2020-2021. <https://doi.org/10.1017/CBO9780511840531>
- [17] Daróczy, László, Gábor Janiga, Klaus Petrasch, Michael Webner, and Dominique Thévenin. "Comparative analysis of turbulence models for the aerodynamic simulation of H-Darrieus rotors." *Energy* 90 (2015): 680-690. <https://doi.org/10.1016/j.energy.2015.07.102>
- [18] Lintermann, Andreas. "Computational meshing for CFD simulations." *Clinical and Biomedical Engineering in the Human Nose: A Computational Fluid Dynamics Approach* (2021): 85-115. https://doi.org/10.1007/978-981-15-6716-2_6